Electrochemistry Communications 114 (2020) 106676

Contents lists available at ScienceDirect

Electrochemistry Communications

journal homepage: www.elsevier.com/locate/elecom

The initiation and formation of a double-layer phosphate conversion coating on steel

Congcong Jiang[a], Zidong Gao[b], Hong Pan[c], Xin Cheng[a,*]

[a] University of Jinan, Jinan 250022, China
[b] Jinan Zhongwei Detection Technology CO. LTD, Jinan 250031, China
[c] Shandong Province Laboratory For Quality Supervision & Test of Cement, Jinan 250022, China

ARTICLE INFO

Keywords:
Alloy steel
Phosphate conversion coating
Amorphous layer
Crystalline layer

ABSTRACT

Although phosphating technology is developing all the time, the formation of phosphate chemical conversion (PCC) coatings still requires further study, particularly in terms of the subcrystalline and/or amorphous base layer at the bottom of the coating. The present study provides some additional insights into the mechanism of formation of a PCC coating on alloy steel using field emission SEM (FE-SEM), X-ray photoelectron spectroscopy (XPS) and X-ray diffractometry (XRD). The results indicate that the PCC coating has a double-layer structure, namely an amorphous base layer in contact with the steel substrate, and an outer crystalline phosphate layer. The formation of the PCC coating can be divided into four stages: electrochemical dissolution of the substrate, deposition of an amorphous phase, phosphate crystallization and growth, and the dynamic balance between coating dissolution and formation.

1. Introduction

Phosphate conversion technology can provide metals with protective surface coatings composed of dielectric and insoluble phosphates [1–7]. The development of phosphate-coated steels began with a British patent of 1869 granted to Ross [8]. Phosphate chemical conversion (PCC) coatings usually have excellent binding performance due to chemical bonding between the coating and the matrix metal [9,10]. In addition, this coating technology is simple and easy to operate at low cost, and the resulting coatings have desirable corrosion resistance. Thus, phosphate conversion technology has been widely used in many fields, including the chemical industry, metallurgy, and the automobile, aerospace and shipbuilding sectors [1,11]. It is well known that a continuous growth of phosphates occurs during the formation of PCC coatings, due to chemical and electrochemical reactions at the metal surface [1,2,12]. When a piece of steel is dipped into an acid conversion bath, many micro primary cells (including microanodes and microcathodes) are formed. The dissolution of iron at microanodes and the evolution of hydrogen at microcathodes can change the pH at the interface between the steel and the bath, then promote the multistage hydrolysis of soluble primary phosphates in the bath to obtain the phosphate ion (PO_4^{3-}). Subsequently, the insoluble phosphate from PO_4^{3-} and the cation (Zn^{2+}, Fe^{2+}, Ca^{2+}) from the bath are deposited on the surface of the steel and then gradually grow to produce a PCC coating [13–15].

However, a few researchers [1,12] have suggested that a very thin base layer is formed first, as soon as the steel makes contact with the conversion bath, and this base layer may contain subcrystalline oxides and phosphates of iron. Crystalline phosphates are then deposited on the subcrystalline layer until finally an intact PCC coating covers the matrix steel. Although the formation mechanism related to PCC coatings on steel and other metals has already been discussed in depth [2,16–18], most studies have focused on the crystalline nature and growth of insoluble phosphates within the PCC coating. The majority of experimental data does not support the presence of a subcrystalline base layer. However, the study reporting a subcrystalline or amorphous base layer has attracted great interest in recent years.

The present study provides some additional insight into the suggested amorphous base layer of a PCC coating on alloy steel using field emission SEM (FE-SEM), X-ray photoelectron spectroscopy (XPS) and X-ray diffractometry (XRD). The aim is to contribute to a comprehensive understanding of the process of forming a PCC coating on the surface of a steel substrate.

* Corresponding author at: Shandong Provincial Key Laboratory of Preparation and Measurement of Building Materials, University of Jinan, No. 336 Nanxinzhuang West Road, Jinan 250022, China.
E-mail address: ujn_chengxin@163.com (X. Cheng).

https://doi.org/10.1016/j.elecom.2020.106676
Received 12 December 2019; Received in revised form 19 January 2020; Accepted 29 January 2020
Available online 30 January 2020

2. Experimental

2.1. Preparation of PCC coating

35CrMnSi alloy steels with the chemical composition 0.35 C, 1.16 Si, 0.82 Mn, 1.17 Cr, 0.01 S, 0.022 P and balance Fe were used as substrate materials. Prior to PCC processing, the alloy steels were abraded using emery paper, degreased in 80 g/L NaOH solution, pickled in 30 ml/L H_3PO_4 and activated in a Ti colloid solution (3 g/L $Na_4Ti(PO_4)_2$). The steels were then immersed in a PCC bath (pH = 2.75 ± 0.05) composed of zinc oxide (25 g/L), phosphoric acid (15 ml/L) and nitric acid (30 ml/L) as well as composite accelerators (2 g/L $NaClO_3$ and 5 g/L $C_6H_8O_7$), for a specified period of time at room temperature. Finally, the PCC-coated coupons were cleaned using deionized water and then dried by air blowing.

2.2. Characterization of PCC coating

The morphology of the PCC coatings was characterized using a SU-70 field emission SEM (FE-SEM). The phase compositions were analyzed using a Rigaku D/max-γB X-ray diffractometer (XRD) using CuKα radiation, operated at 40 kV and 100 mA with a scan speed of 4°/min. In addition, the chemical compositions of the coating were probed using an ESCALAB 250 X-ray photoelectron spectrometer (XPS) with Al Kα radiation (1487 eV) at a power of 150 W, and the data were analyzed using XPSPEAK 4.0 software. An open circuit potential (OCP) versus time curve was recorded from the moment of immersion in the PCC bath for a period of 1800 s using a CHI 660E electrochemical workstation.

3. Results and discussion

3.1. Microstructure and composition

Fig. 1 displays the surface morphology of a sample immersed in the PCC bath for 60 s. Some plate-like crystals had formed on the steel, with an average size of 4–6 μm, as shown in Fig. 1a. It is notable that the plate-like crystals seemed to be embedded at the base which presented a loose network structure (Fig. 1b). It is inferred that the PCC coating consists of a loose base layer in contact with the steel substrate, and an outer crystalline layer. This result was consistent with the previous report that a very thin subcrystalline layer was initially formed when the metal was attacked by the PCC bath, and a crystalline layer of phosphates built up rapidly on this lower layer [1]. Meanwhile, XRD results have shown that the PCC coating consists of both crystalline and amorphous phases, as depicted in Fig. 2. It can be seen that the crystalline phase was composed of hopeite ($Zn_3(PO_4)_2{\cdot}4H_2O$) and

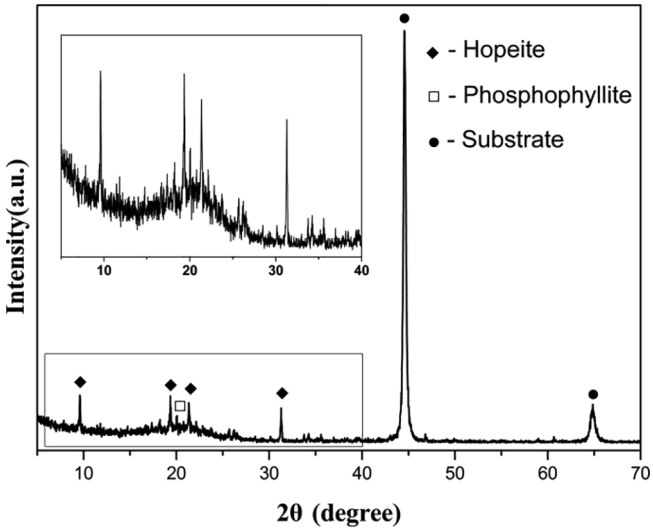

Fig. 2. XRD pattern of a sample after immersion in the PCC bath for 60 s. The insert shows an enlargement of the boxed section of the pattern.

phosphophyllite ($Zn_2Fe(PO_4)_2{\cdot}4H_2O$), while the amorphous phase was most likely due to the loose network structure at the base, which will be discussed in more detail in Section 3.2. It is therefore suggested that the PCC coating was possibly composed of an amorphous base layer and an outer crystalline layer.

3.2. Initial coating on steel

Fig. 3 shows the surface morphology of PCC coatings on steel with conversion times of 10 s and 20 s. The surface of the PCC-coated sample immersed in the bath for 10 s still showed the loose network structure and no crystalline structure was obvious (Fig. 3a), while there were some irregular particles on the surface which could be due to the deposition of sediments in the bath. Regarding the specimen immersed in the bath for 20 s, it can be seen that many small plate-like crystals were formed, with an average size of 0.5–1.0 μm (Fig. 3b), and the base also exhibited a loose network structure. It has therefore been demonstrated that a loose network structure is formed rapidly in the early stage of the treatment process, and small plate-like crystals are subsequently formed on the network structure.

In order to further explain the loose network structure on the surface of PCC-coated steel immersed for 10 s, an XPS survey spectrum of the sample was obtained (see Fig. 4). The XPS results indicated that the coating contained predominantly Fe, O, Zn, P and C elements. The high-

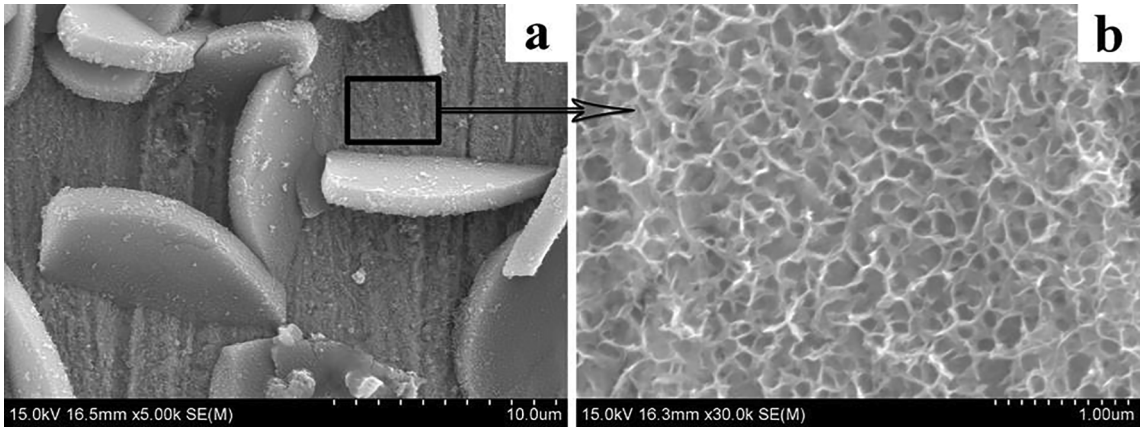

Fig. 1. FE-SEM images of a sample after immersion in the PCC bath for 60 s: (a) at low magnification and (b) higher magnification of the area outlined by the box in (a).

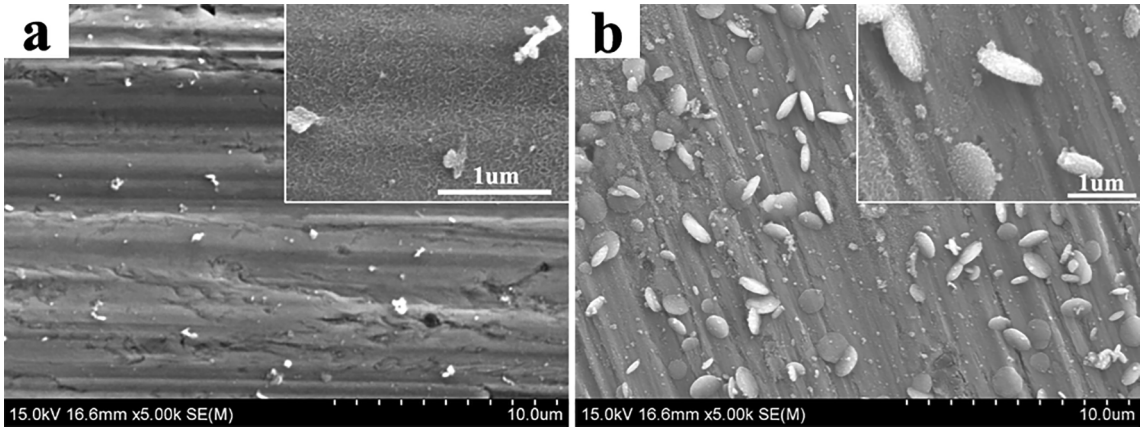

Fig. 3. FE-SEM images of samples after immersion in the PCC bath for (a) 10 s and (b) 20 s. The insets are higher magnification images.

resolution spectrum of C 1 s had a peak at 284.6 eV, which is common in XPS analysis due to adventitious hydrocarbons from the environment [14]. The high-resolution spectra of Fe, Zn and O were further analyzed to elucidate the detailed structure of the coating using the Shirley background correction method (Fig. 4b–d). The high-resolution spectrum of Fe 2p3/2 can be divided into two peaks: one at 710.8 eV and another at 712.6 eV (Fig. 4b), which correspond to γ-Fe_2O_3 [19] and $FePO_4$ [20], respectively. Fig. 4c illustrates that the high-resolution spectrum of weak Zn 2p3/2 has a peak at 1021.9 eV, which could be explained by the presence of Zn. Because some of the Fe in the steel is oxidized during the conversion process, this might cause reduction of some of the Zn^{2+} ions near the surface to Zn, which is deposited on the surface [21]. However, the content of Zn in the coating is so small that it is not detectable by XRD. The high resolution spectrum of O 1 s displays two peaks: one at 530.0 eV and another at 531.5 eV (Fig. 4d). The results demonstrate the presence of Fe_2O_3 and $FePO_4$, which is in good agreement with that of Fe 2p3/2. The intensity of the P 2p peak is weak owing to the low concentration of $FePO_4$. Based on these analyses, it can be concluded that the network base layer is composed of Fe_2O_3 and $FePO_4$.

3.3. Growth of crystals

Fig. 5 depicts the surface topography of the PCC coatings produced on steel after longer conversion times. After immersion in the bath for 1 min (see Fig. 5a), most of the substrate had a sparse coverage of small plate-like crystals. Fig. 5b–e show the growth of the PCC coating after immersion times of 3, 5, 8 and 10 min, respectively. At this stage, a variation in the crystal size occurred, which implied the occurrence of secondary recrystallization, leading to the reappearance of new small

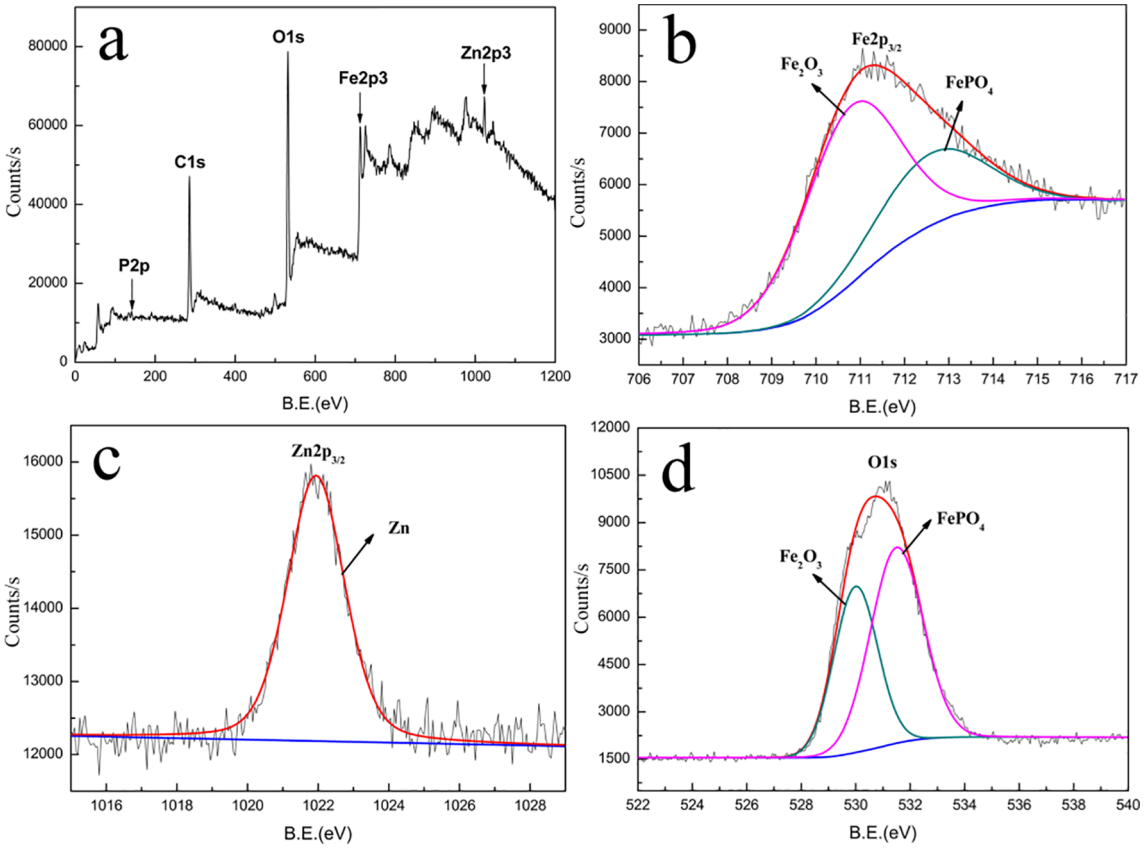

Fig. 4. (a) The XPS survey spectrum and the XPS spectrum of (b) Fe $2p_{3/2}$, (c) Zn $2p_{3/2}$ and (d) O 1 s for samples immersed in the PCC bath for 10 s.

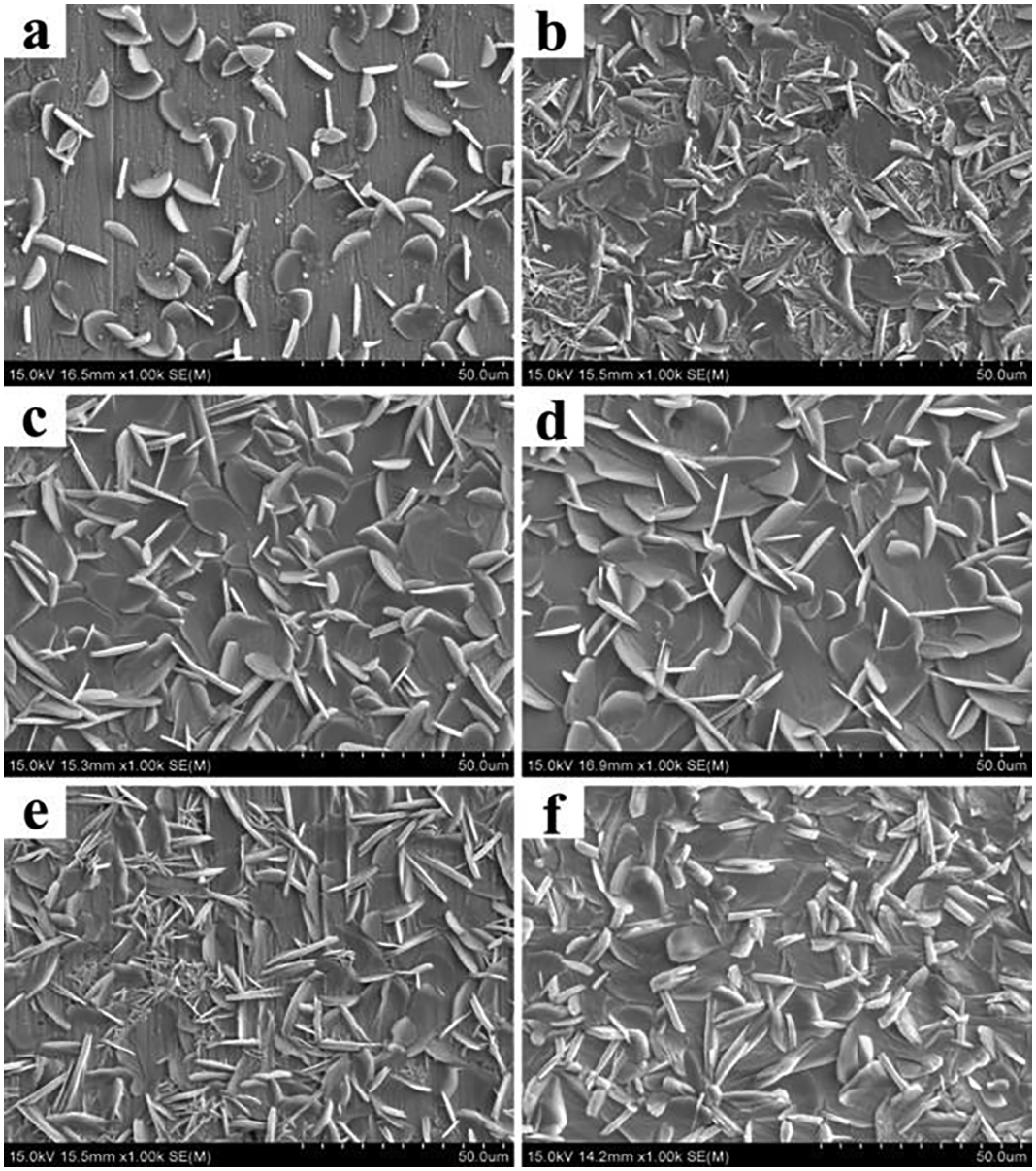

Fig. 5. FE-SEM images of samples after immersion in the PCC bath for (a) 1 min, (b) 3 min, (c) 5 min, (d) 8 min, (e) 10 min and (f) 15 min.

crystals. These small crystals grew quickly to form large plate-like crystals. After immersion for 15 min (Fig. 5f), the surface was fully covered by interweaved slab-like phosphate crystals and the PCC coating became more compact.

3.4. Mechanism of formation of the PCC coating

The formation of a PCC coating on a steel substrate depends on a complicated set of chemical and electrochemical reactions near the substrate surface [16,17]. According to Machu and others [1,11], the formation process can be divided into four phases: the electrochemical dissolution of the substrate; deposition of an amorphous phase; phosphate crystallization and growth; and crystal reorganization. Fig. 6 shows a schematic illustration of the formation of a PCC coating on steel as proposed in this study.

(1) Electrochemical dissolution of steel

When steel is immersed in the acidic PCC bath, a microgalvanic couple is established immediately, as shown in Fig. 6a. The dissolution of iron at microanodes and hydrogen evolution at microcathodes occurs simultaneously via the following reaction:

$$Fe + 2H^+ \rightarrow Fe^{2+} + H_2\uparrow \quad (1)$$

Hydrogen evolution increases the pH at the metal/solution interface, which then alters the dissociation equilibrium, leading to the formation of PO_4^{3-}.

$$H_3PO_4 \rightarrow H_2PO_4^- + H^+ \quad (2)$$

$$H_2PO_4^- \rightarrow HPO_4^{2-} + H^+ \quad (3)$$

$$HPO_4^{2-} \rightarrow PO_4^{3-} + H^+ \quad (4)$$

(2) Deposition of an amorphous phase

It has been reported that a very thin base layer is produced during the first few seconds when the metal (Fe) comes into contact with the PCC bath and is attacked. The film contains oxides and phosphates of iron, which are most likely iron oxide and ferrous phosphate [1]. In principle, when steel is immersed in a dilute phosphoric acid solution, a

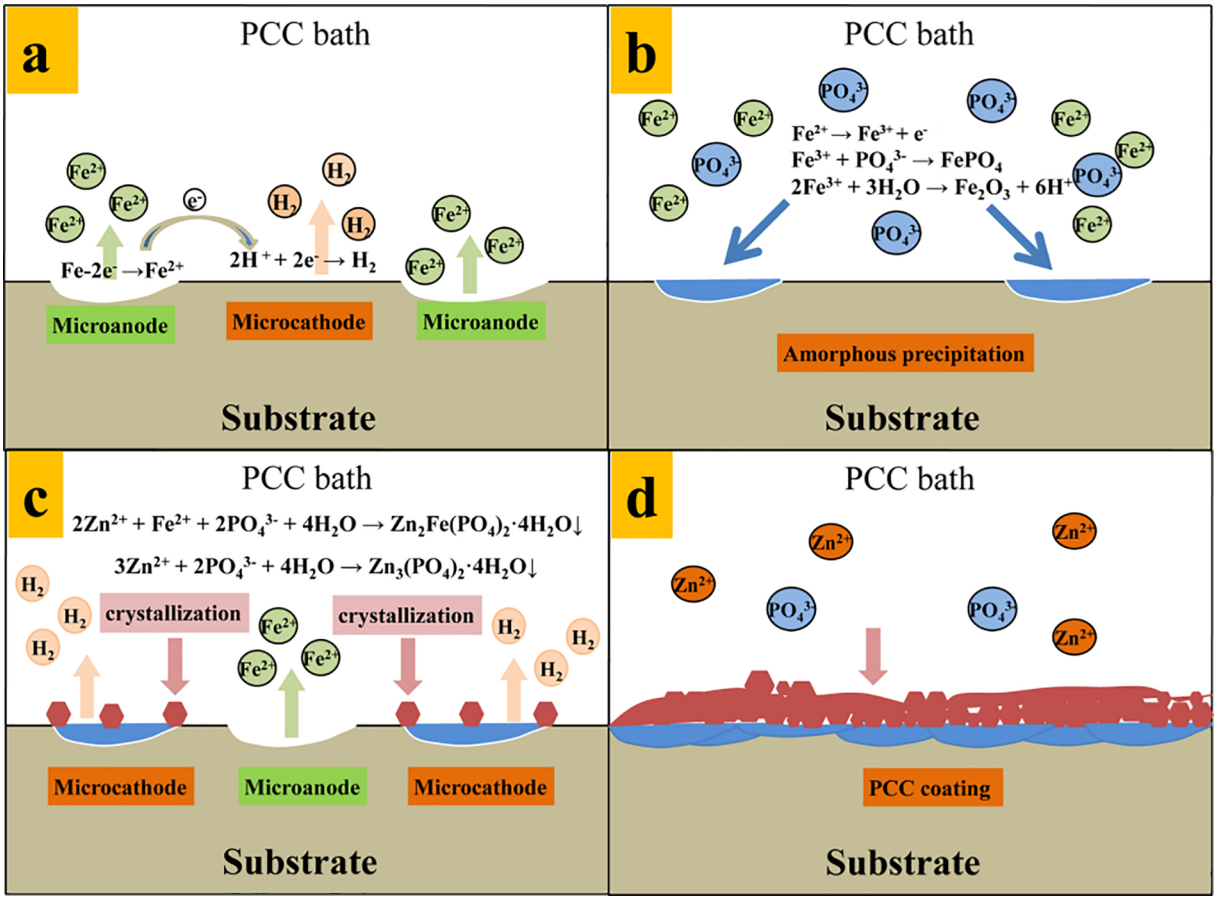

Fig. 6. Schematic diagram of the formation of a PCC coating on steel.

layer of ferrous phosphate is immediately formed [2,18]. However, due to the abundant Fe^{2+} exposed on the surface during the early stages in an acidic PCC bath with added accelerators, $FePO_4$ and Fe_2O_3 are rapidly formed and act as an amorphous base layer on steel. The dissolved Fe^{2+} is rapidly oxidized to Fe^{3+} by accelerators in the PCC, resulting in the rapid precipitation of amorphous ferric phosphate and ferric oxide on the steel surface (Fig. 6b).

$$Fe^{2+} \rightarrow Fe^{3+} + e^{-} \quad (5)$$

$$Fe^{3+} + PO_4^{3-} \rightarrow FePO_4 \quad (6)$$

$$2Fe^{3+} + 3H_2O \rightarrow Fe_2O_3 + 6H^{+} \quad (7)$$

Therefore, the base layer bonds chemically with the substrate, and provides high adhesion between the entire coating and the substrate. The amorphous precipitation process occurs very quickly and is accompanied by substrate dissolution.

(3) Crystallization and crystal growth

When the originally active microanodes have been completely covered by the amorphous base layer, their potential increases compared with the original microcathodes and are then transformed into the present microcathodes. As the bath becomes saturated with PO_4^{3-} and metal ions (Zn^{2+} and Fe^{2+}), insoluble phosphate is deposited and then crystallizes onto the PCC coating on the amorphous base layer (Fig. 6c).

$$2Zn^{2+} + Fe^{2+} + 2PO_4^{3-} + 4H_2O \rightarrow Zn_2Fe(PO_4)_2 4H_2O\downarrow \quad (8)$$

$$3Zn^{2+} + 2PO_4^{3-} + 4H_2O \rightarrow Zn_3(PO_4)_2 4H_2O\downarrow \quad (9)$$

Upon the formation of phosphate crystal nuclei, expansive crystal growth occurs, forming coarse crystals on which some small crystals grow due to recrystallization. This results in a significant decline in porosity.

(4) The dynamic balance of coating dissolution and formation

It is known that the pH at the metal/solution interface can change during the overall conversion process [9,22]. Thus, the coating is continually being dissolved and reformed. In the early stages, coating formation is much faster than dissolution, but as the conversion time increases, the rate of coating formation gradually decreases. Throughout the early stages, the substrate is covered with a loose PCC coating, and thus the PCC bath easily migrates to the coating and reaches the substrate surface at exposed sites. Then, metal dissolution and coating formation occur continuously, which gradually improves the coating and increases its density. When a dynamic balance between coating dissolution and formation is established, a complete PCC coating is formed, as shown in Fig. 6d.

When the sample is immersed in the acid PCC bath, the potential of the metal surface continually changes, accompanying the formation of the coating. Thus, the overall coating formation process could be followed by monitoring the open circuit potential (OCP) as a function of immersion time. The potential–time curve of 35CrMnSi steel obtained from OCP measurements is shown in Fig. 7, which further indicates the various stages of PCC coating formation. In stage I, the potential rapidly shifts to a minimum value of −703 mV, which corresponds to the electrochemical attack on steel in the acid bath. In stage II, the jump in potential from −703 mV to −693 mV implies the rapid formation of a coating, including the precipitation of an amorphous layer followed by

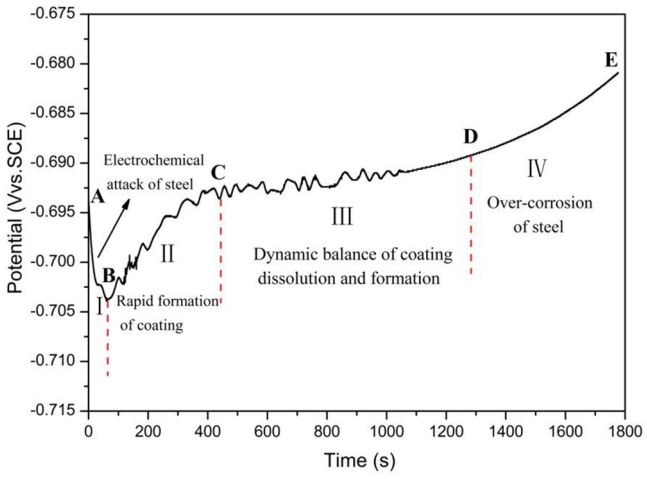

Fig. 7. Open circuit potential of steel as a function of immersion time in the PCC bath.

crystallization and growth. In stage III, the potential stabilizes at approximately −693 mV after an immersion time of 450 s, which indicates that a dynamic balance between coating dissolution and formation has been established, and then the PCC coating is completely formed after about 1200 s. In stage IV, an excessive conversion time may result in the over-corrosion of the coating and steel substrate in the acidic PCC bath. In conclusion, the different stages in the formation of a PCC coating on steel are as follows: electrochemical attack on the steel, rapid formation of the coating, and finally, dynamic balance of coating dissolution and formation.

4. Conclusions

This study analyzes the formation of the phosphate chemical conversion (PCC) coating on alloy steel, particularly the amorphous base layer at the bottom of the coating. The results showed that the PCC coating consists of a double-layer structure, namely an amorphous base layer in contact with the steel substrate, and an outer crystalline phosphate layer. The crystalline layer is mainly composed of hopeite ($Zn_3(PO_4)_2{\cdot}4H_2O$) with phosphophyllite ($Zn_2Fe(PO_4)_2{\cdot}4H_2O$), while the amorphous base layer contains Fe_2O_3 and $FePO_4$. The process of formation of the PCC coating is also described. In the first step, the substrate surface is preferentially dissolved in an acid PCC bath, accompanied by the deposition of an amorphous phase. This is followed by the formation of phosphate crystals on the amorphous base layer. Finally, the PCC coating is gradually improved until a dynamic equilibrium between coating dissolution and formation is established.

CRediT authorship contribution statement

Congcong Jiang: Conceptualization, Investigation, Writing - original draft. **Zidong Gao:** Methodology, Investigation, Data curation. **Hong Pan:** Investigation, Writing - review & editing. **Xin Cheng:** Supervision, Writing - review & editing, Project administration.

Declaration of Competing Interest

The authors declare that they have no known competing financial interests or personal relationships that could have appeared to influence the work reported in this paper.

Acknowledgements

This work was supported by Shandong Provincial Natural Science Foundation of China (ZR2018LE004), Major Basic Research Program of Shandong Provincial Natural Science Foundation of China (ZR2018ZC0741) as well as National Natural Science Foundation of China (51632003), the Taishan Scholars Program, Case-by-Case Project for Top Outstanding Talents of Jinan.

References

[1] T.S.N. Sankara Narayanan, Surface pretreatment by phosphate conversion coatings – a review, Rev. Adv. Mater. Sci. 9 (2005) 130–177.
[2] J. Bogi, R. Macmillan, Phosphate conversion coatings on steel, J. Mater. Sci. 12 (1977) 2235–2240.
[3] X. Zhang, G.-Y. Xiao, B. Liu, C.-C. Jiang, Y.-P. Lu, Influence of processing time on the phase, microstructure and electrochemical properties of hopeite coating on stainless steel by chemical conversion method, New J. Chem. 39 (2015) 5813–5822.
[4] X. Zhang, G.-Y. Xiao, C.-C. Jiang, B. Liu, N.-B. Li, R.-F. Zhu, Y.-P. Lu, Influence of process parameters on microstructure and corrosion properties of hopeite coating on stainless steel, Corrosion Sci. 94 (2015) 428–437.
[5] X.C. Zhao, G.Y. Xiao, X. Zhang, H.Y. Wang, Y.P. Lu, Ultrasonic induced rapid formation and crystal refinement of chemical conversed hopeite coating on titanium, J. Phys. Chem. C 118 (2014) 1910–1918.
[6] X. Zhang, G.Y. Xiao, Y. Jiao, X.C. Zhao, Y.P. Lu, Facile preparation of hopeite coating on stainless steel by chemical conversion method, Surf. Coat. Technol. 240 (2014) 361–364.
[7] C. Jiang, X. Cheng, Anti-corrosion zinc phosphate coating on building steel via a facile one-step brushing method, Electrochem. Commun. 109 (2019) 106596.
[8] W. Ross, Preserving metals from oxidation, British Patent No. 3119, (1869).
[9] N.V. Phuong, K. Lee, D. Chang, M. Kim, S. Lee, S. Moon, Zinc phosphate conversion coatings on magnesium alloys: a review, Met. Mater. Int. 19 (2013) 273–281.
[10] J.E. Gray, B. Luan, Protective coatings on magnesium and its alloys — a critical review, J. Alloy. Compd. 336 (2002) 88–113.
[11] L.Y. Niu, Z.H. Jiang, G.Y. Li, C.D. Gu, J.S. Lian, A study and application of zinc phosphate coating on AZ91D magnesium alloy, Surf. Coat. Technol. 200 (2006) 3021–3026.
[12] S. Adjerid, H.P. Hivart, J.-P. Bricout, J. Oudin, M. Traisnel, Seizure resistance of phosphated coatings influence of carbon content and metallurgical structure of plain carbon steels, Lubr. Sci. 7 (1995) 345–364.
[13] B. Liu, X. Zhang, G.-Y. Xiao, Y.-P. Lu, Phosphate chemical conversion coatings on metallic substrates for biomedical application: a review, Mater. Sci. Eng., C 47 (2015) 97–104.
[14] Y. Song, D. Shan, R. Chen, F. Zhang, E.-H. Han, Formation mechanism of phosphate conversion film on Mg–8.8Li alloy, Corrosion Sci. 51 (2009) 62–69.
[15] W. Zhou, D. Shan, E.-H. Han, W. Ke, Structure and formation mechanism of phosphate conversion coating on die-cast AZ91D magnesium alloy, Corrosion Sci. 50 (2008) 329–337.
[16] J. Flis, J. Mańkowski, T. Zakroczymski, T. Bell, The formation of phosphate coatings on nitrided stainless steel, Corrosion Sci. 43 (2001) 1711–1725.
[17] P.-E. Tegehall, N.-G. Vannerbert, Nucleation and formation of zinc phosphate conversion coating on cold-rolled steel, Corrosion Sci. 32 (1991) 635–652.
[18] U. Takao, O. Taijiro, O. Keiichi, Crystal growth of phosphate coating on iron and steel, Bull. Chem. Soc. Jpn. 42 (1969) 1304–1307.
[19] A.P. Grosvenor, B.A. Kobe, M.C. Biesinger, N.S. McIntyre, Investigation of multiplet splitting of Fe 2p XPS spectra and bonding in iron compounds, Surf. Interface Anal. 36 (2004) 1564–1574.
[20] Y. Wang, P.M.A. Sherwood, Iron (III) phosphate ($FePO_4$) by XPS, Surf. Sci. Spectra 9 (2002) 99–105.
[21] R. Zeng, Z. Lan, L. Kong, Y. Huang, H. Cui, Characterization of calcium-modified zinc phosphate conversion coatings and their influences on corrosion resistance of AZ31 alloy, Surf. Coat. Technol. 205 (2011) 3347–3355.
[22] C.-C. Jiang, G.-Y. Xiao, X. Zhang, R.-F. Zhu, Y.-P. Lu, Formation and corrosion resistance of phosphate chemical conversion coating on medium carbon low alloy steel, New J. Chem. 40 (2016) 1347–1353.